Electrostatics of nanowire transistors with triangular cross sections

Daryoosh Vashaee and Ali Shakouri[a)]
Jack Baskin School of Engineering, University of California, Santa Cruz, California 95064-1077

Joshua Goldberger, Tevye Kuykendall, Peter Pauzauskie, and Peidong Yang
Department of Chemistry, University of California Berkeley, Berkeley, California 94720–1460

(Received 22 August 2005; accepted 27 December 2005; published online 13 March 2006)

The electrostatic properties of nanowire field effect transistors with triangular cross sections were investigated. The Poisson equation was solved for these structures; furthermore, two properties of the nanowire field effect transistors, the gate capacitance and current versus gate voltage, were calculated. The simulation results yielded the type, mobility, and concentration of the carriers, as well as the Ohmic contact resistance of the wire transistor. We examined how wire capacitance depends on various parameters: wire diameter, gate oxide thickness, charge density, and shape. It is shown that the capacitance of a triangular nanowire is less than that of a cylindrical nanowire of the same size, which could be significant in structures with thin gate oxides. The simulation results were compared with the previously reported experimental data on GaN nanowires. © *2006 American Institute of Physics*. [DOI: 10.1063/1.2168229]

INTRODUCTION

There have been a variety of efforts to produce materials based on semiconductor nanostructures such as nanowires[1–6] (NWs) and carbon nanotubes (NTs),[7–13] both of which can provide superior electrical and mechanical properties. These one-dimensional structures have electrical and optical properties that can be used as building blocks in nanoscale devices such as field effect transistors, sensors, and light-emitting diodes. A major focus of these efforts has been on one-dimensional field effect transistor[14–20] applications in which semiconducting nanostructures are used as conducting channels in field effect transistors. The physical attributes of these field-effect transistors (FETs), such as switching speeds, power consumption, etc., must be studied to find out if a nanowire transistor can operate better than other transistor types. Currently, most of the emphasis is to test basic notions about how dimensionality and size influence the physical properties of nanowire transistors and how they could serve as critical building blocks for promising nanoelectronics or nanosensor applications.[21–25] The electrical transport properties of these wires are particularly important since controllable and predictable conductance is vital to many nanoscale electronics applications.

In this paper, we analyze some basic electrostatic properties of semiconductor nanowires with triangular cross sections. We specifically focus on gallium nitride nanowires.[26] These devices were synthesized via metal-initiated metal-organic chemical vapor deposition. Field-emission scanning electron microscopy (FE-SEM) has been used to investigate the length and shape of these nanowires. The GaN nanowires were then connected with two electrodes (source and drain) for this transport study.[26] Drain current as a function of drain-source voltage at different gate biases (V_g) were characterized. These data are used for the verification of our simulation results.

[a)]Electronic mail: ali@ucsc.edu

NANOWIRE CAPACITANCE

We simulated the fabricated triangular GaN nanowire transistor in Ref. 26. The gallium nitride nanowire was synthesized via metal-initiated metal-organic chemical vapor deposition by Kuykendall *et al.*.[26] For comparison, we also considered electrostatic of cylindrical nanowires of the same size. Although the calculations are for GaN nanowire transistors, the general conclusion should apply to other transistors with one-dimensional channels.

The equilibrium potential profile and charge density were obtained by solving the Poisson equation in Cartesian coordinates. In a finite difference solution of the given partial differential equation, an equally spaced grid is set to cover the domain. The solution of the resulted finite difference equations is then obtained iteratively using Gauss-Seidel method. The accuracy is limited by the discretization approximation and roundoff errors that can be reduced down to practical purposes by setting finer grids.[27] The charge density per unit length on the nanowire $Q_L(z)$ is calculated by numerically integrating the electric displacement vector on a Gaussian surface, a closed surface enclosing the total charge. The Gaussian surface must include both charges in the nanowire and the charges induced at the SiO_2/air interface. One may choose an area of the Gaussian surface far enough from the nanowire where induced charges practically vanish. This situation is shown in Fig. 1. In this plot Δ is the distance of the Gaussian surface from the nanowire. It can be seen that with the presence of the dielectric material, the total charge enclosed by the Gaussian surface decreases, which results in a smaller capacitance. The actual capacitance is the smallest (saturated) value in the plot. To set the boundary conditions for the Poisson equation solution, since the nanowire is sitting on an oxide layer and the bias is applied to the substrate, it is assumed that the nanowire is one equipotential surface and the bottom boundary is another. The boundaries at the right hand side, left hand side, and top should be "free." That means the derivative of the potential is zero (Neumann

 © 2006 American Institute of Physics

Downloaded 29 Aug 2007 to 128.32.205.190. Redistribution subject to AIP license or copyright, see http://jap.aip.org/jap/copyright.jsp

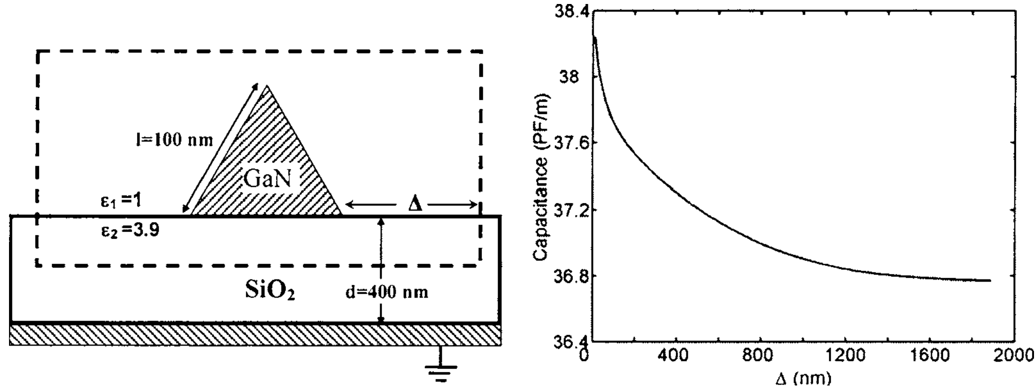

FIG. 1. Left: schematic picture of the nanowire capacitor and the Gaussian surface (dotted line). Right: the calculated capacitance based on different Gaussian surfaces (oxide thickness=400 nm; nanowire width=100 nm).

boundary conditions). The boundary conditions on the sides and top of the device affect considerably the final calculated capacitance. Dirichlet boundary conditions for these surfaces can make the convergence of the numerical calculations faster. However, it turned out that this assumption does not provide an accurate solution.

The final results for the cylindrical nanowire were verified with the known analytical formula:

$$C \approx \frac{2\pi\varepsilon_r^{\mathrm{av}}\varepsilon_0}{\ln[(4h+a)/a]}, \tag{1}$$

where h is the dielectric thickness and a is the width of the GaN nanowires.[28] It is noted that $\varepsilon_r^{\mathrm{av}} \approx 0.5\varepsilon_r^{\mathrm{SiO_2}}(=1.95)$ since the dielectric material occupies only the space below the nanowire.

Figure 2 shows the calculated capacitance versus the width of the nanowire (i.e., the diameter for the cylindrical wire and the side width for the triangular nanowire). For comparison two cases of capacitors, one with the dielectric material (air/SiO_2) and one without the dielectric material (air/air), are assumed. It can be seen that the approximate formula has the adequate accuracy for both cylindrical and triangular nanowires with h=400 nm. The calculated potential profile of the given structure is shown in Fig. 3. The left plot shows the calculated equipotential surfaces around the GaN triangular nanowire. The right plot shows the calculated potential along a line within the dielectric material (SiO_2) and parallel to the x axis in a distance Δ below the nanowire. We assume that the nanowire width is 100 nm and the oxide thickness is 400 nm. It can be seen that the potential vanishes rapidly with distances from the nanowire.

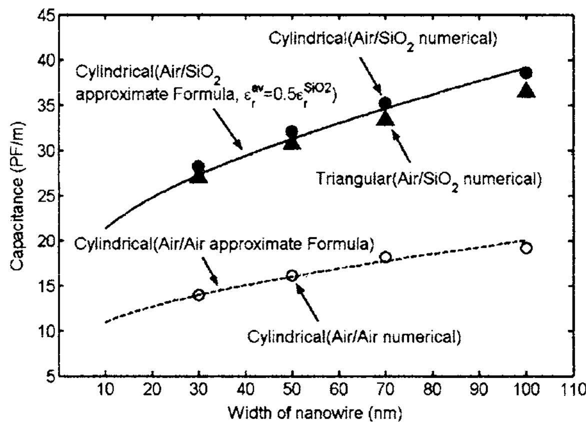

FIG. 2. Calculated capacitance vs nanowire width. The solid and dotted curves show the calculation results using the approximate formula for cylindrical air/air and air/SiO_2 capacitors, respectively. The symbols show the results of the numerical calculations for cylindrical air/air (open circles), cylindrical air/SiO_2 (solid circles), and triangular air/SiO_2 (triangles) capacitors (oxide thickness=400 nm).

To check the effect of gate oxide thickness, the capacitance per unit length versus wire diameter is numerically calculated for different oxide thicknesses (50–400 nm) and is plotted in Fig. 4. For comparison, the capacitance of a cylindrical nanowire with the same dimension is also plotted. It is seen that the difference between the triangular and cylindrical geometry would be larger for thinner oxides (h <100 nm). It is also seen that the triangular nanowire capacitance has less dependence on wire diameter and its value is smaller than the cylindrical one. Therefore, using the analytical formula (1), which is derived for cylindrical nanowires, overestimates the capacitance of triangular nanowires with thin oxides ($h<100$ nm).

The expression used for the nanowire capacitance is based on the assumption that the nanowire is an equipotential surface like in metals. However, the presented GaN nanowire has relatively low doping concentration ($\sim 4\times10^{18}$ cm^{-3}). Thus, this nanowire is not perfectly metallic and the expression used for the nanowire capacitance may not be quite accurate. A more accurate expression for the nanowire capacitance is given by Krčmar *et al.*[29] where they calculate the capacitance for an infinitely long coaxial cable of nonideal conductors. However, our structure of interest is a triangular nanowire above a dielectric substrate as shown in Fig. 1–left. We will estimate the capacitance with that of a long cylinder replacing the triangular nanowire as before. Following a similar analysis as of Krčmar *et al.*,[29] the potential inside the cylindrical conductor is derived by solving the Poisson equation as

$$\phi_{\mathrm{in}}(\rho) = AI_0(k_b\rho) - \frac{\delta\tilde{\mu}_b}{e}, \tag{2}$$

where $I_n(x)$ is the nth order modified Bessel function and A is a constant. $\delta\tilde{\mu}_b$ is the shift in the bulk electrochemical potential, e is the electron charge, and ρ is the distance from

Downloaded 29 Aug 2007 to 128.32.205.190. Redistribution subject to AIP license or copyright, see http://jap.aip.org/jap/copyright.jsp

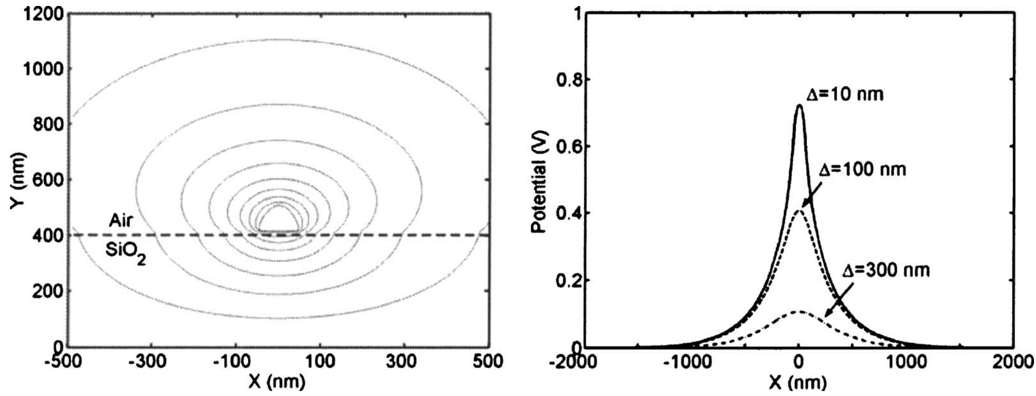

FIG. 3. Calculated potential profile of a triangular nanowire. The left plot shows the equipotential surfaces and right plot shows the calculated potential along a line within the dielectric material (SiO_2) and parallel to the x axis in a distance Δ below the nanowire (oxide thickness=400 nm).

the center of the cylinder. k_b is called the inverse of the bulk screening length and is defined Eq. (3) as

$$k_b \equiv \left(\frac{\varepsilon_0 \varepsilon_r^{\text{in}}}{e^2} \left. \frac{\partial \mu_b}{\partial n_b} \right|_{n_{b0}} \right)^{-1/2}. \tag{3}$$

Here μ_b is the bulk chemical potential and n_b is the local electron number density. Gauss' law gives the change in the electrostatic potential on the symmetry line outside the tube due to the charge per unit length of $\delta\lambda$ as

$$\phi_{\text{out}}(\rho) = \frac{\delta\lambda}{2\pi\varepsilon_r^{\text{out}}\varepsilon_0} \ln\left(\frac{2h+a-\rho}{\rho}\right), \tag{4}$$

where a is the diameter of the cylinder. The constants A and $\delta\tilde{\mu}_b$ are determined from the $\rho=a/2$ boundary conditions: $\phi_{\text{in}}=\phi_{\text{out}}$ and $\varepsilon_r^{\text{in}}\partial\phi_{\text{in}}/\partial\rho=\varepsilon_r^{\text{out}}\partial\phi_{\text{out}}/\partial\rho$. The capacitance per unit length for the nonideal conductors is then calculated as

$$\frac{C}{L} = -e\frac{\delta\lambda}{\delta\tilde{\mu}_b} = 2\pi\varepsilon_r^{\text{av}}\varepsilon_0\left[\ln\left(\frac{4h+a}{a}\right) + \frac{2}{\varepsilon_r^{\text{in}}k_b a}\frac{4h+2a}{4h+a}\frac{I_0(k_b a/2)}{I_1(k_b a/2)}\right]^{-1} \approx 2\pi\varepsilon_r^{\text{av}}\varepsilon_0\left[\ln\left(\frac{4h}{a}\right) + \frac{2}{\varepsilon_r^{\text{in}}k_b a}\frac{I_0(k_b a/2)}{I_1(k_b a/2)}\right]^{-1} \quad \text{if } a \ll h. \tag{5}$$

Here $\varepsilon_r^{\text{in}}$ is the GaN dielectric constant that is about 10. We have also used an average dielectric constant, $\varepsilon_r^{\text{av}}$, for $\varepsilon_r^{\text{out}}$ as in Eq. (1). In order to calculate the variation of chemical potential with density, we have assumed the effective mass of wurtzite GaN material to be $0.22m_e$. Figure 5 shows the calculated capacitance versus the width of the nanowire for different doping concentrations. $\varepsilon_r^{\text{av}}$ and h are assumed to be 1.95 and 400 nm, respectively. We have also assumed a three-dimensional (3D) density of state for the calculation of the bulk screening length.

It is interesting to see that the metallic approximation is valid even down to a doping concentration of $\sim 10^{17}$ cm^{-3}. However, the capacitance value starts to deviate from the metallic assumption at lower doping concentrations and this is more significant for narrow nanowires ($a < 30$ nm).

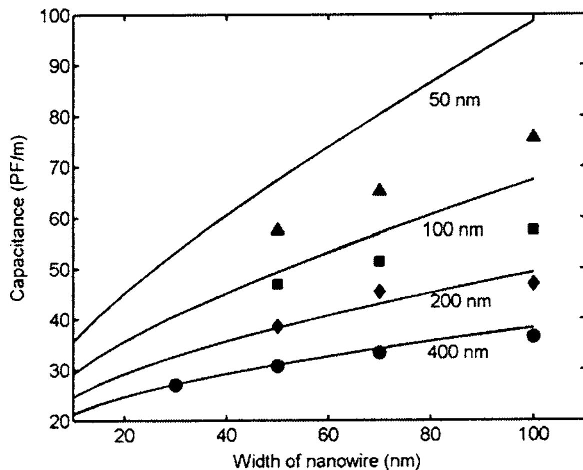

FIG. 4. Calculated capacitances of the triangular (symbols) and cylindrical (solid lines) nanowire vs nanowire width for different oxide thicknesses (50, 100, 200, and 400 nm).

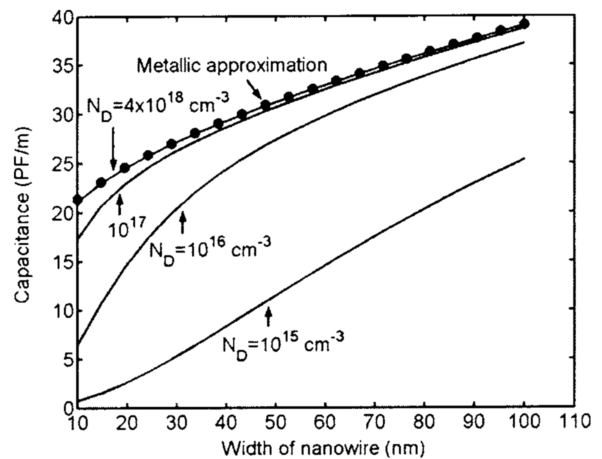

FIG. 5. Calculated gate oxide capacitance for various doping concentrations of the GaN nanowire.

Downloaded 29 Aug 2007 to 128.32.205.190. Redistribution subject to AIP license or copyright, see http://jap.aip.org/jap/copyright.jsp

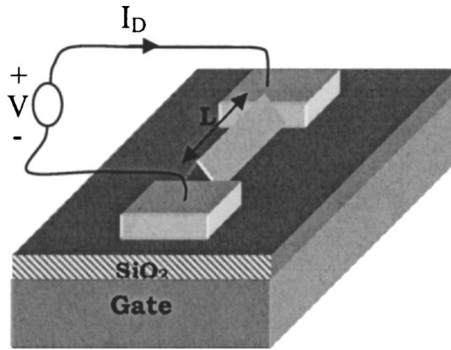

FIG. 6. Schematic picture of the GaN nanowire transistor.

NANOWIRE TRANSISTOR

Another important issue that is studied in this section is the transport properties of the nanowire transistor. The transport properties of the triangular nanowire have been investigated using a backgated two-probe scheme (Fig. 6) in Ref. 26. The current (I_D) versus both source-drain voltage (V_{DS}) and gate voltage (V_{GS}) was measured to determine the type, mobility, and concentration of the carriers. In general, the nanowire conductance increases for V_g greater than zero and decreases for V_{GS} less than zero, indicating that these metal-organic chemical vapor deposition (MOCVD)-derived GaN wires are n type.[26] Figure 7 shows the experimental data from Ref. 26. It is possible to estimate the carrier mobility from the transistor transconductance in linear region using Eq. (6),

$$I_D \cong \mu \frac{C}{L^2}(V_{GS} - V_{th})V_{DS}, \tag{6}$$

where μ is the carrier mobility, V_{th} is the threshold voltage of the transistor, C is the capacitance, and L is the length of the GaN nanowire ($L \approx 12.8$ μm for this case).

As it is shown in Fig. 7, I_D saturates at large values. This is due to the high contact resistance (R_C) at the metal electrodes that starts to dominate the total resistance of the device at high current values.

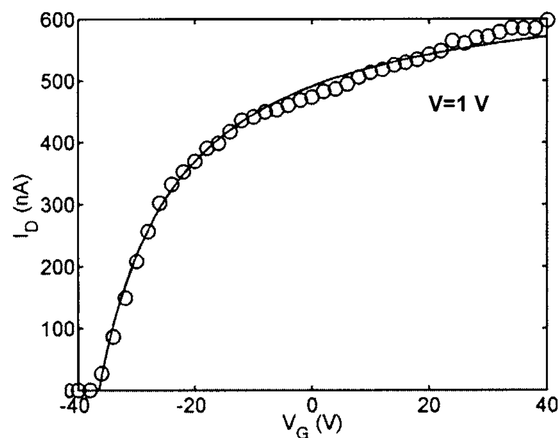

FIG. 7. Drain current as a function of gate voltage (V_G) for the GaN nanowire. The circled and solid curves show the measured data and theoretical fit, respectively. Gate capacitance is calculated numerically and is equal to 27 pF/m. Nanowire length (L) and width (a) are 6.4 μm and 30 nm, respectively.

$$V = V_{DS} + 2R_c I_D. \tag{7}$$

From the IV plot of the transistor in Fig. 7, the calculated gate capacitance ($C \approx 27$ pF/m for $a=30$ nm from Fig. 2), and Eqs. (6) and (7), mobility and contact resistance of the nanowire transistor can be determined. The simulation result is also shown in Fig. 7.

Mobility and contact resistances are determined to be 118 cm^2/V s and 743 kΩ, respectively. Similar contact resistances are reported for nanotubes in the literature.[30,31] This mobility is almost two times the 65 cm^2/V s value reported in Ref. 26, which is due to the consideration of the contact resistance in our calculations. Extra charges such as fixed and mobile charges inside SiO_2, and charges in surface states of the NW can affect the threshold voltage. These three types of charge can be identified by the standard measurement of the low and high frequency capacitances.[32] However, such nonideal charges only shift the threshold voltage. The voltage shift due to mobile charges inside SiO_2 varies with the drain current due to the voltage drop across the contact resistances. This can change the slope of the IV plot in Fig. 7 as well, which is ignored in the current analysis. The other nonideal charges only cause a constant shift in the voltage axis of Fig. 7. Thus the calculated contact resistance and mobility, which appear in the slope of the plot, remain unaffected.

CONCLUSION

The electrostatic properties of nanowires with triangular cross sections were explored. Important properties of the field effect nanowire transistor such as the wire capacitance and the transistor transconductance were calculated by solving the Poisson equation. The theoretical and experimental results of the current versus source-drain voltage and gate voltage of the GaN nanowire transistor were compared and the carrier mobility and Ohmic contact resistance of the transistor were determined. The capacitance of the triangular NW was compared with that of the cylindrical NW and it was shown that the capacitance of the former structure is noticeably smaller for the transistors with thin gate oxides.

ACKNOWLEDGMENTS

This work was supported by the US Department of Energy and the National Science Foundation.

[1] Y. Xia *et al.*, Adv. Mater. (Weinheim, Ger.) **15**, 353 (2003).
[2] M. S. Gudiksen, L. J. Lauhon, J. Wang, D. C. Smith, and C. M. Lieber, Nature (London) **415**, 617 (2002).
[3] M. S. Sander, A. L. Prieto, Y. M. Lin, R. Gronsky, A. M. Stacy, T. D. Sands, and M. S. Dresselhaus, Mater. Res. Soc. Symp. Proc. **635**, C4.36.1-6 (2001).
[4] Y. Cui, X. Duan, J. Hu, and C. M. Lieber, J. Phys. Chem. B **104**, 5213 (2000).
[5] A. S. Barnard, S. P. Russo, and I. K. Snook, Nano Lett. **3**, 1323 (2003).
[6] X. Duan, Y. Huang, and C. M. Lieber, Nano Lett. **2**, 487 (2002).
[7] For a review on CNTs, see M. S. Dresselhaus, G. Dresselhaus, and P. C. Eklund, *Science of Fullerences and Carbon Nanotubes* (Academic, San Diego, CA, 1996).
[8] S. Iijima, Nature (London) **354**, 56 (1991).
[9] S. Tans, A. Verschueren, and C. Dekker, Nature (London) **393**, 49 (1998).
[10] S. J. Wind, J. Appenzeller, R. Martel, V. Derycke, and Ph. Avouris, Appl. Phys. Lett. **80**, 3817 (2002).

Downloaded 29 Aug 2007 to 128.32.205.190. Redistribution subject to AIP license or copyright, see http://jap.aip.org/jap/copyright.jsp

[11]V. Derycke, R. Martel, J. Appenzeller, and Ph. Avouris, Nano Lett. **1**, 453 (2001).
[12]R. Martel, V. Derycke, C. Lavoie, J. Appenzeller, K. K. Chan, J. Tersoff, and Ph. Avouris, Phys. Rev. Lett. **87**, 256805 (2001).
[13]S. Rosenblatt, Y. Yaish, J. Park, J. Gore, V. Sazonova, and P. L. McEuen, Nano Lett. **28**, 869 (2002).
[14]J. Chen and R. Könenkamp, Appl. Phys. Lett. **82**, 4782 (2003).
[15]S. J. Tans, A. R. M. Verschueren, and C. Dekker, Nature (London) **393**, 49 (1998).
[16]R. Martel, T. Schmidt, H. R. Shea, T. Hertel, and Ph. Avouris, Appl. Phys. Lett. **73**, 2447 (1998).
[17]C. Zhou, J. Kong, and H. Dai, Appl. Phys. Lett. **76**, 1597 (2000).
[18]V. Derycke, R. Martel, J. Appenzeller, and Ph. Avouris, Nano Lett. **1**, 453 (2001).
[19]A. Bachtold, P. Hadley, T. Nakanishi, and C. Dekker, Science **294**, 1317 (2001).
[20]X. Liu, C. Lee, and C. Zhou, Appl. Phys. Lett. **79**, 3329 (2001).
[21]C. M. Lieber, Solid State Commun. **107**, 607 (1998).
[22]J. Hu, T. W. Odom, and C. M. Lieber, Acc. Chem. Res. **32**, 435 (1999).
[23]C. Dekker, Phys. Today **52**(5), 22 (1999).
[24]J. Voit, Rep. Prog. Phys. **57**, 977 (1994).
[25]C. Kane, L. Balents, and M. P. A. Fisher, Phys. Rev. Lett. **79**, 5086 (1997).
[26]T. Kuykendall, P. Pauzauskie, S. Lee, Y. Zhang, J. Goldberger, and P. Yang, Nano Lett. **3**, 1063 (2003).
[27]C. M. Snowden, *Introduction to Semiconductor Device Modeling* London, New York (Springer-Verlag, New York, 1989).
[28]See, for example, P. M. Morse and H. Feshbach, *Methods of Theoretical Physics* (McGraw-Hill, New York, 1953), p. 11. The NW is considered as a metallic cylinder, which is a good approximation as long as the density of states at the Fermi level is high.
[29]M. Krčmar, W. M. Saslow, and A. Zangwill, J. Appl. Phys. **93**, 3495 (2003).
[30]R. Martel, T. Schmidt, H. R. Shea, T. Hertel, and Ph. Avouris, Appl. Phys. Lett. **73**, 2447 (1998).
[31]Y. Cui, Z. Zhong, D. Wang, W. U. Wang, and C. M. Lieber, Nano Lett. **3**, 149 (2003).
[32]B. Streetman and S. Banerjee, *Solid State Electronic Devices*, 5th ed. (Prentice Hall, Englewood Cliffs, NJ, 2000).

Downloaded 29 Aug 2007 to 128.32.205.190. Redistribution subject to AIP license or copyright, see http://jap.aip.org/jap/copyright.jsp